A NEW TOOL FOR SATELLITE RE-ENTRY PREDICTIONS

Arrun Saunders[(1)], Hugh G. Lewis[(2)], Graham G. Swinerd[(3)]

University of Southampton, Highfield, Southampton, SO17 2BJ, UK,
[(1)]Email: a.saunders@soton.ac.uk
[(2)]Email: h.g.lewis@soton.ac.uk
[(3)] Email: g.g.swinerd@soton.ac.uk

ABSTRACT

Satellite drag data plays an important role in the estimation of atmospheric density and the study of thermospheric cooling and contraction. There are many ways of calculating atmospheric density, but inferring thermospheric density from satellite drag data is a relatively cost-effective way of gathering in-situ measurements. Given an initial satellite orbit, one approach is to use an orbital propagator to predict the satellite's state at some time ahead and then to compare that state with the Two-Line Element (TLE) data at the same epoch. The difference between the mean motions from consecutive TLE sets is calculated then compared to results obtained from the orbital propagator. From this an estimate of global average density can then be calculated. The validation of a new orbital propagator that will be used for this purpose is the primary focus of this paper. Here, the validation takes the form of re-entry prediction for decaying satellites.

1. INTRODUCTION

As satellite orbits decay, the orbital altitude decreases such that aerodynamic drag becomes an increasingly dominant factor in perturbing the orbit. To model a satellite's orbit during the time up to its decay, accurate estimates of atmospheric density are very important. A feature used in the orbital propagator that helps increase the predictive power of the re-entry dates is the U.S. Naval Research Laboratory's Mass Spectrometer and Incoherent Scatter Radar empirical atmospheric model from the ground up to the exosphere (NRLMSISE-00). The NRLMSISE-00 provides high accuracy density estimates for use in drag calculations, taking into account many characteristics of the solar-terrestrial environment. Other perturbations included in the orbital propagator model are gravity anomalies (using the Joint Gravity Model JGM3) and luni-solar gravity.

To validate the computer code developed for the orbital propagation of objects orbiting in the thermosphere, TLE data for satellites with U.S. Space Surveillance Network numbers 10973, 20967 and 26873 were used to predict their re-entry date. By taking the final TLE sets published for each satellite and propagating the orbit until the satellite reaches the re-entry altitude of 90 km , a prediction of the satellite's re-entry date is obtained. By analysing the time variation of the predicted re-entry dates compared with the actual re-entry date was the method by which the accuracy of the propagator was established.

As the aim is to evaluate the propagator before using it to predict thermospheric densities from TLE sets, only data that is immediately retrievable or derivable from the TLEs are to be used in this study.

2. THE ORBITAL PROPAGATOR

The orbital propagator works by taking the initial conditions of a satellite, and then propagating its orbit numerically using a 7^{th} order Runge-Kutta-Fehlberg method. Spatially it requires the Cartesian vector components of the satellite's position and velocity relative to the centre of the Earth. Temporally it uses the year and the decimal day of the year of the satellite TLE epoch. Finally a ballistic parameter of the satellite, which will be discussed in greater detail later, is required to estimate the atmospheric drag.

As the source of satellite initial conditions are given by TLEs in the form of classical orbital elements, a conversion to Cartesian vector components was required. This conversion tool comes in the form of the freely available Simplified General Perturbations (SGP) 4 analytical propagator [1]. The SGP4 propagator is the tool by which the TLE sets are initially produced, and due to the unique way in which periodic orbital variations are removed, the conversion back to the Cartesian vectors needs to performed in the exact opposite manner [1]. The output coordinate system of the SGP4 Cartesian vectors uses the True Equator Mean Equinox of Epoch (TEME). Therefore the orbital propagator used for this study was written to use exactly the same system. The date format required by the orbital propagator and that given in the TLE sets are identical, and the ballistic parameter can be estimated with varying accuracy from more than one of the TLE's data fields.

Currently there are four different sources of perturbations that make up the acceleration model for

Proc. '5th European Conference on Space Debris', Darmstadt, Germany
30 March – 2 April 2009, (ESA SP-672, July 2009)

the satellite propagation, which will be discussed separately in the following sections. Additional perturbations are planned to be included. However as the propagator is still in the development stage insufficient time and research has been available to include them in this study.

2.1. Geopotential

For precision orbit determination and prediction, The spherical Earth assumption is too imprecise. To accurately model the acceleration caused by the Earth, coefficients from the Joint Gravity Model (JGM) 3 have been used.

From Vallado [2], the calculation of the geopotential U using the normalised JGM3 coefficients ($\bar{C}$ and $\bar{S}$), the satellite's geocentric latitude φ, longitude λ and distance from the centre of the Earth r is made using

$$U = \nabla \frac{GM}{r} \sum_{n=0}^{\infty} \sum_{m=0}^{n} \frac{R_E^n}{r^n} \bar{P}_{nm} \left(\bar{C}_{nm} \cos(m\lambda) + \bar{S}_{nm} \sin(m\lambda)\right), \quad (1)$$

where ∇ is the gradient function, GM is the Earth's gravitational constant (398,600.4415 km^3/s^2), n and m are the order and degree of the gravitational spherical harmonics respectively, R_E is the equatorial radius of the Earth (6378.1363 km) and $\bar{P}$ is the normalized Legendre polynomial in which the spherical harmonics are expanded in terms of the sine of the geocentric latitude.

2.2. Atmospheric Drag

The acceleration vector on a satellite due to atmospheric drag $\boldsymbol{a}_{aero}$ is calculated from

$$\boldsymbol{a}_{aero} = -\frac{1}{2}\rho v \delta \boldsymbol{V}, \quad (2)$$

where ρ is the local atmospheric density, v is the satellite's scalar velocity, $\boldsymbol{V}$ is the satellite's velocity vector and δ is the ballistic coefficient. Usually, δ is defined as

$$\delta = \frac{C_D A}{m}, \quad (3)$$

where C_D is the satellite's drag coefficient, A is the projected cross-sectional area of the satellite perpendicular to the velocity vector and m is the satellite's mass. However as the only source of satellite information used is from the TLE data, these parameters are not given explicitly and therefore need to be estimated in other ways.

The atmosphere was assumed not to co-rotate with the Earth. This decision was made due to the orbital characteristics of the specific satellites used in the re-entry predictions. Each of the three satellites had orbit inclinations of approximately ~82° meaning they flew over polar latitudes and, from Hedin *et al.* [3], evidence was shown for anti-rotational trends of the upper atmosphere over the poles. With the wind flowing in the opposite direction to the satellite's velocity vector an increase in the relative drag acceleration would be experienced by the satellites as they flew over these latitudes and therefore would lead to an earlier re-entry date than originally predicted. To quantify this, a re-entry prediction using satellite 10973 was conducted using a co-rotating atmosphere, the results of which will be discussed later.

2.3. Luni-Solar Perturbations

To model the perturbations caused by the gravity of the Moon and the Sun, a method which provided continuous ephemeris data was required. Therefore alongside the propagation of the satellite, a second 'luni-solar' propagator runs simultaneously to predict the relative positions of the Earth, Moon and Sun.

The 'luni-solar' propagator uses a 4th order Runge-Kutta numerical integration technique and takes initial conditions from ephemeris data at 10 day intervals obtained from the NASA Horizons System [4]. The positions of the Earth and Moon are then numerically integrated. However as the only bodies involved in the 'luni-solar' propagator are the Earth, Moon and Sun, a different method had to be used in order to accurately predict the Sun's position as the majority of the gravitational perturbations from the rest of the Solar System were missing. The Sun's position was predicted linearly interpolating between the 10 day Horizons' ephemeris data. A maximum displacement error of approximately 20 km over the period between 1950 and 2008 was achieved using this approach.

Once the direction vectors of the Moon and Sun relative to the Earth were obtained, the third body accelerations $\boldsymbol{a}_{3rd\ body}$ were calculated using [5]

$$\boldsymbol{a}_{3rd\ body} = \frac{GMr}{s^3}\left(-\boldsymbol{\varepsilon}_r + 3\boldsymbol{\varepsilon}_s(\boldsymbol{\varepsilon}_s \boldsymbol{\varepsilon}_r)\right), \quad (4)$$

where s is the scalar distance of the perturbing body from the centre of the Earth and $\boldsymbol{\varepsilon}$ is the unit position vector relative to the centre of the Earth of the satellite or perturbing body depending on the subscript r or s respectively.

2.4. Ballistic coefficient.

For all of the re-entry predictions carried out in this study, the ballistic coefficient was calculated using the method described by Hoots & Roerich [1] with the B* drag term, a value given in the TLE sets. From Vallado [2] the constant conversion using this method is given by

$$\delta = 12.741621B^*, \quad (5)$$

where B^* in Eq. 5 is the B* drag term retrieved directly from the TLE data.

As this study is to evaluate and validate the accuracy of the propagator, the initial conditions need to be as similar as possible to those used during the process of predicting thermospheric densities, as the method will follow a similar process. This means that only values derived from the TLE data could be used. To improve the ballistic coefficient estimation, individual satellite characteristics such as mass, shape and material surface properties would be helpful. However in predicting thermospheric densities, thousands of satellite TLEs will be required and to gather individual satellite characteristics would take and impractical amount of time.

When the TLE sets are initially created the B* drag term is used as a fitting parameter to soak up any un-modelled errors in the global force model. In some cases, it can be completely unrelated to drag effects during large variations in other satellite perturbations [2].

In attempting to estimate a sensible value of B* to be used in conjunction with Eq. 5, the variation of each of the satellite's B* values, 200 days prior to re-entry is shown in Fig. 1.

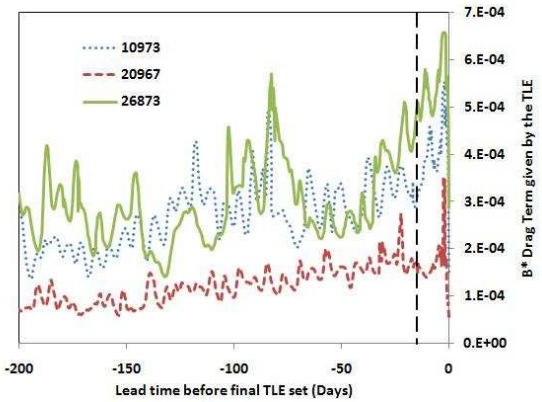

Figure 1. The variation of the B drag term given by the TLE data sets 200 days prior to the final published TLE before re-entry. The vertical dashed line represents this study's prediction epoch 15 days before re-entry.*

As can be seen from Fig. 1, the B* drag term varies significantly, especially during the last 15 days before re-entry (the time in which predictions for this study were made), and as B* gives a poor representation, only a very crude estimation could be made of the actual ballistic coefficient. Therefore, the median value of B* for the last 15 days for each satellite was used. For the actual values used, Tab. 1 shows the maximum, minimum and median values of B* for all 3 satellites during the last 15 days before re-entry.

Table 1. The maximum, minimum and median values of the B drag term from TLEs for the last 15 days before re-entry for each satellite.*

Satellite	**10973**	**20967**	**26873**
Maximum	5.5345E-4	3.5519E-4	6.5701E-4
Minimum	1.3750E-4	5.6173E-5	1.4160E-4
Median	3.4548E-4	2.0568E-4	3.9931E-4

As the variation of the drag coefficient can vary by as much as ±20% [6], three cases were conducted for each re-entry prediction for each satellite, with the ballistic coefficient varying by ±20%.

2.5. Thermospheric Density

To calculate the acceleration due to atmospheric drag, the NRLMSISE-00 empirical atmospheric model [7] was used to estimate the local air density. This model uses inputs of the satellites geocentric position, the date and time of day, solar flux data in the form of the F10.7 cm radio flux and the geomagnetic index, a_p, for varying times prior to the date given. The daily indices for both the F10.7 cm solar flux and geomagnetic index were given by National Oceanic and Atmospheric Administration (NOAA) [8]. The orbital propagator linearly interpolates a continuous value between the available daily data. This was done to eliminate input step changes when the orbital integration time moves over one day and the F10.7 flux value changes from one to the next. Similarly, the geomagnetic a_p index values were linearly interpolated to provide a moving average between the published 3-hourly indices.

3. RESULTS

For each satellite studied, the re-entry prediction dates are shown in Figs. 2-4. In addition to the cases where the ballistic coefficients were derived from the B* drag term, the effect of varying the ballistic coefficient by ±20% are plotted alongside the original curves.

In Figs. 2-5 the vertical dashed lines represent the epochs of the TLE sets used to predict the resulting re-entry dates.

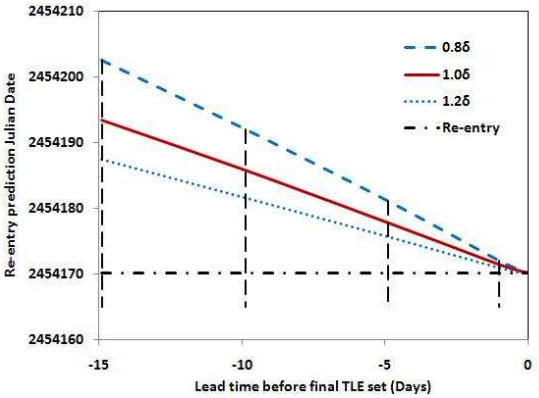

Figure 2. 10973 Re-Entry Time Windows.

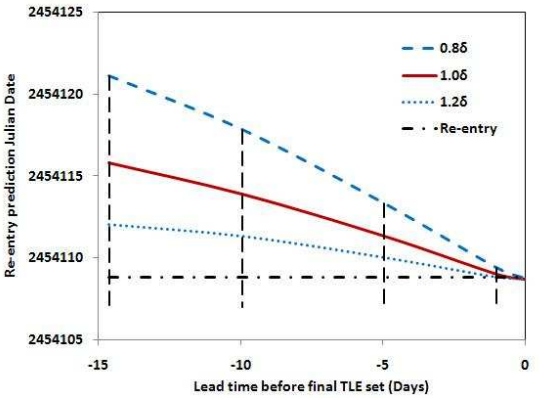

Figure 3. 20967 Re-Entry Time Windows.

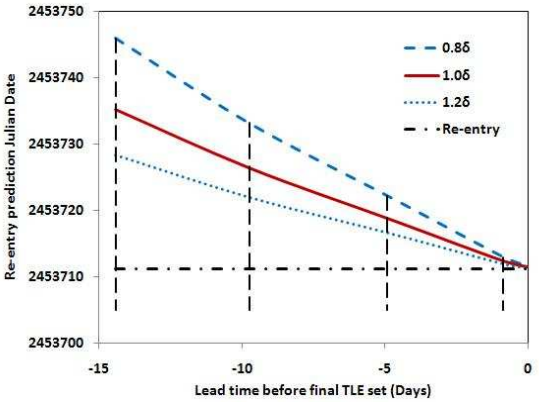

Figure 4. 26873 Re-Entry Time Windows.

4. COMPARISONS

During the initial stages of this study, comparisons of various factors were done to further understand the working of the orbital propagator. For each comparison carried out, a curve was plotted on the same graph (see Fig. 5) in order to clearly show the impact of each factor.

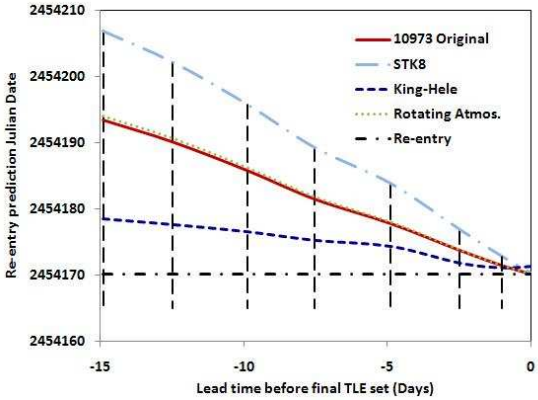

Figure 5. The comparisons between changing the various factors of ballistic coefficient and atmospheric rotation for satellite 10973.

4.1. AGI's Satellite Tool Kit

For a check of whether the output given by the propagator is reasonable, a comparison was carried out with the AGI software 'Satellite Tool Kit' (STK) version 8. The Astrogator propagator within this software gives the user the ability to pick and choose which perturbation is to be included and from which source the data is obtained. Therefore, to match the orbital propagator, the gravity model JGM3 was chosen along with the atmospheric density model of the NRLMSISE-00 as well as third body lunar and solar perturbations. For the flux indices, an average F10.7 cm flux of 70 (10^{-22}J/sec m^2 Hz) was approximated from the actual flux data of the epoch along with an a_p index of 2.5 (nT). The comparison was done using satellite 10973 and the results of the prediction re-entry dates are shown in Fig. 5 as 'STK8'.

4.2. Ballistic Coefficient

Currently an investigation is being carried out into using a different method to predict the ballistic coefficient. From King-Hele [9], the ballistic coefficient can be calculated by

$$\delta = -\frac{\dot{a}\mu}{a^2 \rho v^3}, \tag{6}$$

where $\dot{a}$ is the rate of change of the orbital semi-major axis, μ is the gravitational constant of the Earth (398,600.4415 km^3/s^2), ρ is the local density assuming a spherically symmetric exponential atmosphere and v is the speed of the satellite relative to the atmosphere.

In accordance with King-Hele's method, the density of a spherically symmetric exponential atmosphere is defined by

$$\rho = \rho_{p0} \exp\left\{\frac{r_{p0} - r}{H}\right\}, \quad (7)$$

where r is the scalar distance of the satellite from the centre of the Earth, the subscript 'p0' denotes density values at perigee and distance, and H is the scale height,

$$\frac{1}{H} = \frac{Mg}{RT} - \frac{2}{r_0}. \quad (8)$$

Here M is the molecular weight of the ambient atmosphere, g is the acceleration due to gravity, R is the gas constant (8314 J/kg mol K) and T is the ambient atmospheric temperature (K). Both the molecular weight and the ambient temperature can be obtained from the output of the NRLMSISE-00 model. The temperature is given explicitly but the molecular weight needs some calculation. The NRLMSISE-00 gives outputs of number densities per unit volume of each species of gas at a user-specified altitude. Knowing the number densities N_n and atomic/molecular masses α_n of all the significant species, the molecular weight of the ambient atmosphere is calculated by

$$M = \frac{(\alpha_1 N_1 + \alpha_2 N_2 + \alpha_3 N_3 + \ \ldots + \alpha_n N_n)}{N_{TOTAL}}, \quad (9)$$

where N_{TOTAL} is the total number of atmospheric gas particles.

In Eqs. 6 & 7, the Cartesian components of distance and velocity of the satellite's orbit are obtained from the output of the SGP4 propagator, therefore remaining inside the criterion of only using data derived from the TLE set. The semi-major axis required in Eq. 6 is derived from the scalar distance and velocity, whereas the rate of change of semi-major axis $\dot{a}$ is calculated using the rate of change of the mean motion given in the first line of the TLEs. Fig. 6 shows the comparison of the ballistic coefficients of King-Hele's method against that calculated directly from the B* drag term.

The results of the re-entry predictions suggests that the ballistic coefficient was underestimated, which is no great surprise considering the poor representation the B* gives of the actual drag parameter, therefore the estimation of the ballistic coefficient given by King-Hele's method would imply a more accurate prediction of re-entry dates as shown in Fig. 5 as 'King-Hele'.

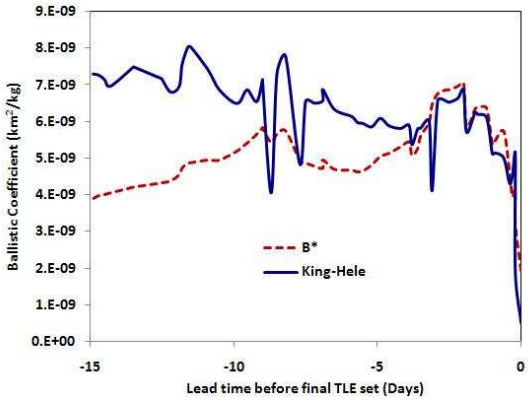

Figure 6. A comparison of the ballistic coefficient calculated directly from the B drag term given by the TLE data and that calculated by King-Hele's method.*

4.3. Atmospheric Rotation

To model a co-rotating atmosphere, the assumption was made that there was no *z*-component of wind velocity. The coordinate system used is Earth centred with the *z*-axis, parallel to the Earth's spin axis, pointing North. The wind velocity vector was then subtracted from the satellite's velocity vector given in Eq. 2.

For a co-rotating atmosphere, the acceleration due to atmospheric drag would actually be lower than the case of a static atmosphere, as the wind component would be in the same direction as the satellite, thus reducing the relative air velocity and drag experienced by the satellite. The case of a co-rotating atmosphere in the orbital propagator is demonstrated using the same conditions as the re-entry predictions used for satellite 10973, with the predicted re-entry dates shown in Fig. 5 under 'Rotating Atmos.'. As can be seen, the re-entry dates are all slightly later during the 15 day lead time, therefore supporting the idea that a simple co-rotating atmospheric model would not be sufficient.

Further development of the orbital propagator will add an empirical wind model to improve orbital predictions.

5. CONCLUSIONS

For all satellite re-entry predictions the dates were later than the actual re-entry. This was believed to be due to the use of the B* drag term used to calculate the ballistic coefficient. To predict re-entry dates more accurately using the propagator, a much better model of the ballistic parameter is required, as well as more information about the specific satellites.

The differences between the three ballistic coefficients (±20%) showed good convergence as the lead time

decreased. This suggested that the handling of atmospheric drag within the orbital propagator is behaving as expected. It appears that the modelling of the ballistic parameter is the prime factor in accurately predicting re-entry dates and, as such, requires more investigation before the propagator is used to predict thermospheric densities.

In validating the working of the code, the results from this study are more than satisfactory, especially when comparing with the 'exact' same acceleration model as used with the STK program.

6. REFERENCES

1. Hoots, F.R. and Roehrich, R.L., (1980). *Propagation of NORAD Element Sets*, Spacetrack Report No. 3, Project Spacetrack, Aerospace Defence Command, United States Air Force, Colorado Springs, Colorado, USA.

2. Vallado, D.A., (2007). *Fundamentals of Astrodynamics and Applications*, Hawthorne, CA: Microcosm Press, New York NY: Springer.

3. Hedin, A.E., Spencer, N.W. and Killeen, T.L., (1988). *Empirical Global Model Of Upper Thermosphere Winds Based On Atmosphere And Dynamics Explorer Satellite Data*, Journal Geophysical Research, Vol. 93, No. A9, pp 9959-9978.

4. Yeomans, D. K. (2009). NASA Horizons System. *http://ssd.jpl.nasa.gov/?horizons*.

5. Montenbruck, O. and Gill, E., (2005). *Satellite Orbits: Models, Methods, Applications*, Springer, Berlin Heidelberg New York.

6. Pardini, C. and Anselmo, L., (2001). *Re-entry Predictions In Support Of The Inter-Agency Space Debris Co-ordination Committee Test Campaigns*, Proceedings of the Third European Conference on Space Debris, ESOC, Darmstadt, Germany, pp 521-526.

7. Picone, J. M., A. E. Hedin, D. P. Drob, and A. C. Aikin, (2002), *NRLMSISE-00 Empirical Model Of The Atmosphere: Statistical Comparisons and Scientific Issues*, J. Geophys. Res., 107, No. A12, pp 1468.

8. Erwin, E.H., (2007) NOAA Indices. *ftp://ftp.ngdc.noaa.gov/*.

9. King-Hele, D., (1987), *Satellite Orbits in an Atmosphere: Theory and Applications*, Blakie, Glasgow.